Journal of Geoscience and Environment Protection, 2026, 14(4), 229-245
https://www.scirp.org/journal/gep
ISSN Online: 2327-4344
ISSN Print: 2327-4336

Classification and Application of Surrounding Rock Stability in Mining Roadways of Gently Inclined and Inclined Coal Seams

Chaoyang Dong*, Zhihai Ji, Ziqi Zhou, Yangwei Di

College of Mine Safety, North China Institute of Science and Technology, Beijing, China
Email: *1349185349@qq.com

How to cite this paper: Dong, C. Y., Ji, Z. H., Zhou, Z. Q., & Di, Y. W. (2026). Classification and Application of Surrounding Rock Stability in Mining Roadways of Gently Inclined and Inclined Coal Seams. *Journal of Geoscience and Environment Protection, 14,* 229-245.
https://doi.org/10.4236/gep.2026.144013

Received: January 27, 2026
Accepted: April 24, 2026
Published: April 27, 2026

Abstract

To scientifically and quantitatively evaluate the stability of the surrounding rock in retreat mining roadways at Balianceng Coal Mine, a comprehensive research approach integrating *in-situ* measurements, theoretical analysis, laboratory testing, and numerical simulation was adopted. The geological structure, physical-mechanical properties, and stress state of the surrounding rock were systematically investigated. Based on the stability classification criteria for surrounding rock in gently inclined and inclined coal seam retreat roadways, a set of comprehensive evaluation indices governing roadway stability was established, enabling a systematic quantitative classification of surrounding rock stability grades. An optimized support scheme was then proposed according to the classification results, and field application demonstrated satisfactory support performance. The results indicate that the roof of the No. 26 coal roadway at Balianceng Coal Mine is composed mainly of a composite medium-hard rock assemblage consisting of silty mudstone and argillaceous sandstone, while the floor is dominated by a single medium-hard silty mudstone. The coal seam exhibits a firmness coefficient of 0.90, the surrounding rock contains a moderate density of structural discontinuities, the mining-induced influence coefficient is 2.18, and the ratio of the maximum horizontal principal stress to the vertical stress is 1.33. Based on the comprehensive evaluation, the surrounding rock of the No. 26 coal roadway is classified as Class III, corresponding to a moderately stable condition. The proposed methodology provides a practical reference for applying engineering analogy methods to roadway stability evaluation and support design.

Keywords

Geological Structural Characteristics, Physical and Mechanical Properties, Stress State, Stability Classification, Optimized Support Scheme

1. Introduction

When assessing the potential risk of instability and failure of roadway surrounding rock, the key considerations include the complexity of geological structures, the diversity and integrity of structural features, the inherent physical and mechanical properties of the rock mass, and the *in-situ* stress environment (Zhao et al., 2024; Zhang, 2019). A refined classification of surrounding-rock stability is essential for designing and implementing targeted engineering measures, and its importance has become increasingly prominent as coal resources are progressively exploited at greater depths. Therefore, in-depth investigation of the influencing factors and classification methods of surrounding-rock stability is of great significance for promoting the sustainable development of the coal mining industry (Dong et al., 2023; Feng, 2022).

In academic research, the central task in surrounding-rock stability studies is to elucidate the mechanical response and instability mechanisms of rock masses under excavation disturbance and stress redistribution. Hou et al. (1999) established a surrounding-rock stability classification system for gateroads of retreat-mining faces with dip angles ranging from 8˚ to 45˚, and identified seven key controlling indices, including roof and floor strength, burial depth, first caving interval, and the mining height-to-seam thickness ratio. This system can effectively characterize roadway stability. Xu (2021) investigated the grading of retreat-mining roadway stability from the perspectives of mine-pressure transmission and support-rock interaction, and implemented a numerical classification approach. Ma et al. (2024) developed an evaluation system integrating the Fuzzy Analytic Hierarchy Process and Grey Relational Analysis (FAHP-GRA), constructed a dual-algorithm assessment model for retreat-mining roadways, identified major risk factors affecting stability based on the evaluation results, and proposed targeted risk-control measures. Liu et al. (2024) addressed the pronounced strata-pressure behavior in deep coal-seam roadways and, based on the Kastner formula, conducted an orthogonal numerical simulation considering five factors—roadway height-to-width ratio, lateral pressure coefficient, burial depth, cross-sectional shape, and surrounding-rock strength—followed by analysis of variance and intuitive sensitivity ranking to determine the influence of each factor on roadway deformation and failure. Yin (2015) investigated a case in which a deep roadway intersected a fault zone, analyzed the stress and displacement characteristics and safety indices under different intersection configurations between fault planes and roadway cross-sections, and comprehensively evaluated roadway stability.

In addition, some researchers have applied fuzzy clustering methods to classify known roadway types and incorporate them into surrounding-rock stability evaluation systems (Lian et al., 2023; Duan, 2018; Ding, Qiao, & Zhu,2009). Multivariate (stepwise) regression has also been used to quantify the effects of factors influencing roadway stability, enabling a more accurate assessment of surrounding-rock stability (Zhu et al., 2015; Zhang et al., 2016). However, constrained by the coupled complexity of rock-mass characteristics, stress fields, and geological en-

vironments, existing fuzzy evaluation approaches still rely heavily on empirical judgment, have limited capability for dynamically predicting time-dependent stability, and lack unified and systematic quantitative indices.

Accordingly, this study takes the retreat-mining gateroad in the No. 26 seam at the Baliancheng Coal Mine as the research object and investigates the geological structure and stress distribution characteristics of the surrounding rock. On this basis, a multi-factor comprehensive evaluation of surrounding-rock stability is conducted by integrating stability classification methods for gently inclined and inclined coal-seam roadways. Based on the classification results, a preliminary optimization design of the roadway support scheme is proposed, and a stability grading index system applicable to the mining district is established. The proposed framework can provide theoretical support and engineering guidance for roadway stability evaluation and support design using the engineering analogy method.

2. Geological Structural Characteristics of Surrounding Rock

2.1. Coal-Rock Coring

Taking the No. 26 coal seam in the 72605 return air roadway as the research object, 10 m long core samples collected from this area were analyzed to clarify the structural assemblage characteristics of the roof and floor strata of the roadway. On this basis, laboratory experiments were further conducted to investigate the physical and mechanical properties of the rock. The core samples obtained from the roof and floor are shown in Figure 1 and Figure 2.

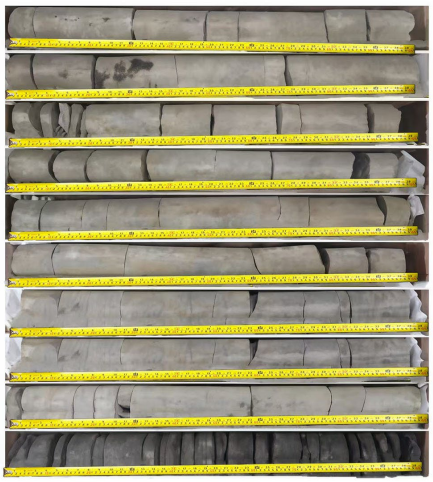

Rock name	Bar chart	Thickness/m	Drill Hole depth/m
coal		0.93	10.00
argillaceous sandstone		5.07	9.07
sandy mudstone		4.0	4.0

Roof-strata core photographs and stratigraphic column for the No. 26 coal

Figure 1. Structural characteristics of roadway roof strata.

As shown in Figure 1, the roof core of the No. 26 coal seam can be divided into three lithological sections with distinctly different characteristics. The interval from 0 to 4.1 m consists mainly of gray sandy mudstone, in which silty particles are uniformly distributed, with a slight coarsening of grains in the middle part, and plant debris fossils are locally observed. Although more than ten core seg-

ments longer than 10 cm were recovered within this section, the overall integrity of the core is poor, exhibiting a fragmented structure.

The section from 4.0 to 9.07 m is dominated by dark gray argillaceous sandstone with evenly distributed argillaceous cement. Horizontal bedding is clearly developed, accompanied by thin interlayers of mudstone, and occasional sandstone interbeds occur in the lower part. The core from this interval also shows a relatively high degree of fragmentation.

The interval from 9.07 to 10.0 m corresponds to black massive semi-bright coal, characterized by irregular fracture surfaces. Due to mechanical disturbance during drilling and the scouring effect of drilling fluids, the integrity of the coal core in this section was significantly damaged, and no intact coal core longer than 10 cm was recovered.

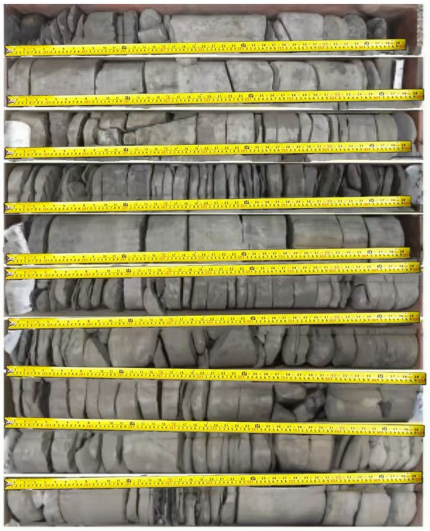

Rock name	Bar chartt	Thickness/m	Drill Hole depth/m
silty mudstone		3.00	10.00
mudstone		1.18	7.00
silty mudstone		3.82	5.72
medium-grained sandstone		1.18	1.90
silty mudstone		0.72	0.72

Floor-Strata Core Photographs and Stratigraphic Column for the No. 26 coal

Figure 2. Structural characteristics of roadway floor strata.

As shown in **Figure 2**, the floor core of the No. 26 coal seam is overall highly fragmented. Within several intervals, including 0.72 - 1.90 m, the rock exhibits a grayish-white color, moderate cementation, and poor sorting. It is composed mainly of quartz and feldspar grains, with a small amount of clay or other cementing materials binding the sand particles into a consolidated rock mass; therefore, these sections are identified as medium-grained sandstone. The overall integrity of the core is poor, and no intact rock segments longer than 10 cm were observed.

Within the ranges of 0 - 0.72 m,1.90 - 5.72 m,7 - 10 m, the rock is mainly gray in color, locally transitioning to dark gray. Silty particles are generally uniformly distributed, with slight grain coarsening in the middle portions, and plant debris fossils are commonly present. The argillaceous components are unevenly distributed, and these sections are identified as silty mudstone. In the interval of 5.72 - 7 m, the rock is predominantly dark gray, with uniformly distributed argillaceous material and thin mudstone interlayers, and is therefore identified as mudstone.

In summary, the thickness distribution of roof lithologies in the No. 26 coal seam shows relatively minor variation. The roadway roof is mainly composed of sandy mudstone and argillaceous sandstone. In contrast, the floor lithology is more complex and exhibits rapid lithological changes, consisting primarily of medium-grained sandstone, silty mudstone, and mudstone.

2.2. Detailed Investigation of Roadway Roof Strata

Two vertical exploratory boreholes with a depth of 8 m were drilled into the roof of the 72605 transportation roadway. A digital borehole panoramic imaging system was employed to inspect and characterize the internal structural features of the rock mass within the boreholes. The imaging results of Borehole No. 1 are presented in Figure 3.

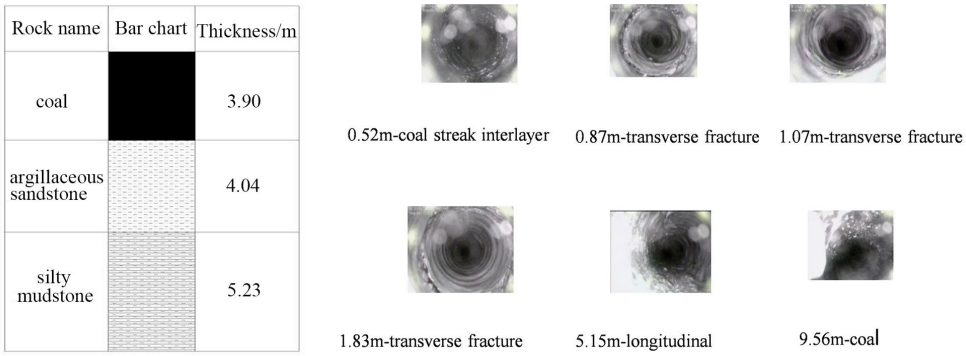

Figure 3. Borehole observation results of roof No. 1.

Based on the roof imaging data obtained from Borehole No. 1, the revealed lithological assemblage is relatively simple, consisting mainly of alternating silty mudstone and argillaceous sandstone, with a single, extremely thin coal interlayer developed locally. Notably, the argillaceous sandstone contains a relatively high proportion of clay minerals.

In terms of specific geological features, interbedded coal seams were identified at borehole depths of 0.52 m and 9.56 m. Within the upper 2.0 m of the roadway roof, multiple transverse fractures are observed, while a longitudinal fracture is developed in the silty mudstone at a depth of 5.15 m, with an extension length of approximately 1.8 m. Overall, the fracture distribution revealed by this borehole exhibits a clear depth-dependent concentration, mainly confined to the zone within 2.0 m above the roadway roof. It is worth noting that the two coal interlayers constitute potential structural weak planes. In addition, seepage has already been observed in the roof area corresponding to this borehole. Considering the scale and distribution of the fractures, the roof fractures at present can be characterized as being at a moderate development level.

The borehole imaging of the No. 2 roof borehole is shown in Figure 4.

Based on the roof imaging data from Borehole No. 2, the revealed lithological structure is relatively simple, consisting mainly of alternating silty mudstone and

argillaceous sandstone. The argillaceous sandstone is characterized by a relatively high clay content.

Detailed geological observations show that transverse fractures are developed at borehole depths of 0.88 m, 1.09 m, and 1.82 m, and multiple transverse fractures are distributed within the zone extending 2.0 m above the roadway roof. Overall, the fractures revealed by this borehole exhibit a pronounced depth-dependent concentration, being mainly confined to the interval within 2.0 m above the roadway roof. In addition, seepage has been observed in the roof area corresponding to this borehole. Considering the scale and distribution of the fractures, the current roof fractures can be characterized as exhibiting a moderate level of development.

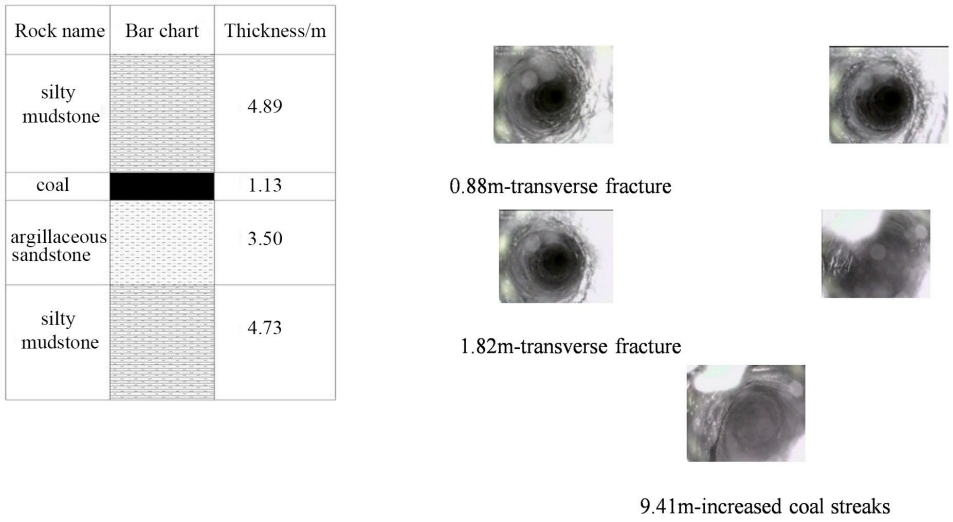

Figure 4. Borehole observation results of roof No. 2.

In summary, the roadway roof is primarily composed of a composite assemblage of silty mudstone and argillaceous sandstone, with a thin coal interlayer of approximately 1.0 m locally developed. Within the 0 - 2.0 m range above the roof, the rock mass is relatively fragmented, forming a fracture zone dominated by transverse fractures. Moreover, longitudinal fractures are developed within the argillaceous sandstone at depths of 5.15 - 6.95 m. Overall, the roof fractures are assessed to be at a moderate stage of development.

2.3. Physical and Mechanical Properties of Roadway Surrounding Rock

Laboratory tests were conducted on coal and rock samples to determine key mechanical parameters, including uniaxial compressive strength, elastic modulus, Poisson's ratio, and cohesion. All tests were performed in accordance with the standard Methods for Determining the Physical and Mechanical Properties of Coal and Rock (GB/T 23561-2009). The test results are presented in Table 1.

Table 1. Physical and mechanical properties of rock specimens.

Lithology	Bulk density (g/cm³)	Compressive strength (MPa)	Elastic modulus (GPa)	Poisson's ratio	Tensile strength (MPa)	Cohesion (MPa)	Internal friction angle (o)
Silty mudstone (Roof)	2.43	53.14	12.49	0.32	1.02	5.61	36.13
Argillaceous sandstone (Roof)	2.40	49.60	9.75	0.35	0.85	3.99	32.33
No. 26 coal	1.33	9.00	2.23	0.43	0.28	2.62	34.28
Silty mudstone (Foof)	2.42	50.63	10.55	0.32	1.02	5.54	35.61

3. Stress State of Roadway Surrounding Rock

3.1. *In-Situ* Stress Measurement

To determine the stress state of the roadway surrounding rock, the hydraulic fracturing method was employed to measure the *in-situ* stress. The measurements were conducted at the R264 survey point of the 72605 transportation roadway in Baliancheng Coal Mine. The measurement boreholes were drilled vertically upward, with the borehole collar located at a burial depth of approximately 590 m.

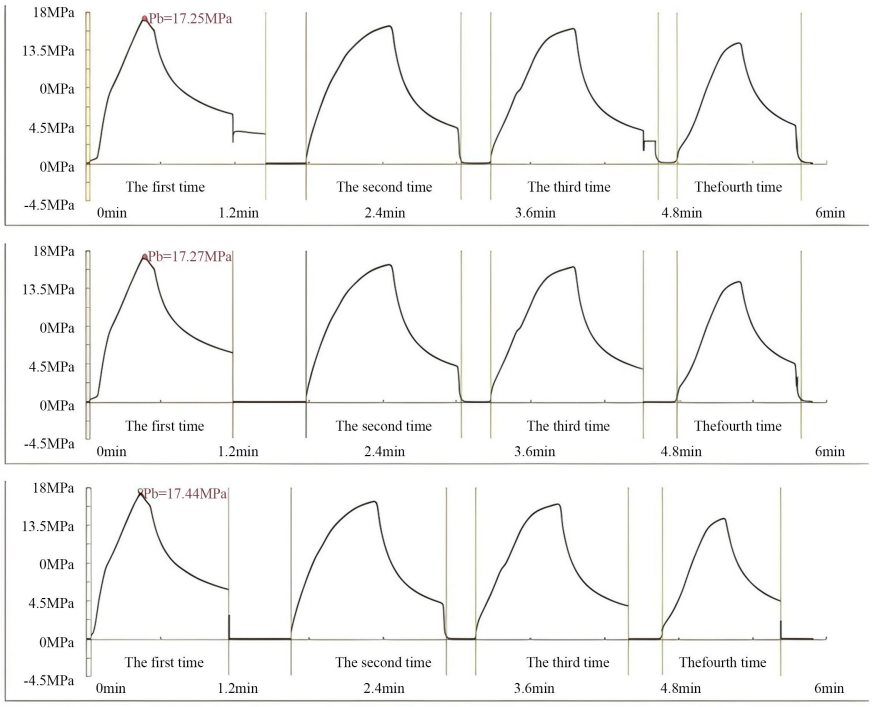

Figure 5. Pressure variation curve of measuring point 3.

A total of three measurement boreholes were arranged, with a spacing of 10 m between adjacent boreholes. Single-interval hydraulic fracturing tests were completed in each borehole. During the fracturing tests, the breakdown pressure, reopening pressure, and fracture closure pressure recorded in different loading-un-

loading cycles exhibited clear and well-defined response characteristics, demonstrating good consistency and repeatability among the boreholes. The detailed measurement results of the three boreholes at Measurement Point No. 3 are presented in Figure 5 and Table 2.

Table 2. Hydraulic fracturing parameters and calculated *in-situ* principal stresses for three boreholes.

Borehole No.	Interval depth m	Fracturing parameters			Principal stress value (MPa)		
		Breakdown pressure, P_b	Re-opening pressure, Pr	Shut-in pressure, Ps	S_H	S_h	S_v
1	590	17.25	12.96	9.01	14.07	9.01	14.01
2		17.27	13.47	10.72	18.69	10.72	
3		17.44	13.39	10.59	18.30	10.59	
Average					17.02	10.10	

1) Pb—*In-situ* Rock Breakdown Pressure; Pr—Fracture Reopening Pressure; Ps—Instantaneous Fracture Surface Pressure; Sh—Minimum Horizontal Principal Stress; SH—Maximum Horizontal Principal Stress; Sv—Vertical Principal Stress. 2) The vertical stress Sv was calculated assuming an average bulk density of the overlying rock mass of 2.5 g/cm^3.

Based on the pressure data listed in Table 2, the maximum and minimum horizontal principal stresses (S_H and S_h) in this area were determined from the fracture reopening pressure and fracture closure pressure, respectively. The calculated values of S_H range from 14.07 to 18.69 MPa, while Sh varies between 9.01 and 10.72 MPa.

According to the thickness of the overlying strata and assuming a rock bulk density of 2.5 g/cm^3, the vertical principal stress (S_V) was calculated to be 14.01 MPa. The resulting stress relationship satisfies $S_H > S_V > S_h$, indicating that the stress field is dominated by horizontal stress.

Borehole imaging was further used to identify the fracture orientations in the three measurement boreholes, as shown in Figure 6. The corresponding orientations of the maximum horizontal principal stress (S_H) are N54.56˚E, N53.55˚E, and N33.67˚E, respectively.

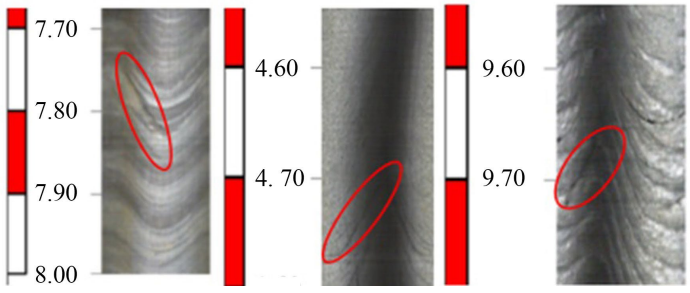

Figure 6. Fracturing fracture.

3.2. Distribution of Mining-Induced Stress

Based on the engineering geological conditions of Baliancheng Coal Mine, a three-dimensional numerical simulation was conducted using FLAC3D to analyze

the mining process of the No. 26 coal seam. During the simulation, the influence of coal seam extraction on the stress field of the surrounding rock was systematically investigated, and the evolution characteristics of the mining-induced stress field during the retreat mining process were obtained.

3.2.1. Model Establishment

Based on the geological conditions of the No. 26 coal seam at Baliancheng Coal Mine, a three-dimensional numerical model with dimensions of 400 m × 500 m × 282 m was established to simulate the mining-induced effects of the coal seam. The model coordinate system was defined such that the x-axis is aligned with the dip direction of the working face and the y-axis with the strike direction. A key refinement zone was defined within 40 m above and below the No. 26 coal seam, where the element size of the coal seam and the immediate roof and floor was refined to 3 m × 3 m × 2 m. Additional mesh refinement was applied along the advance direction of the working face and within its influence zone along the strike to ensure accurate determination of the peak abutment pressure and its spatial extent. The refined model consists of approximately 2.0×10^6 elements, and the mesh quality satisfies numerical requirements, ensuring computational stability.

The bottom boundary of the model was fixed in all directions, while normal displacement constraints were applied to the lateral boundaries in the x and y directions. A vertical stress of 9.725 MPa was applied to the top boundary to represent the overburden load. The Mohr-Coulomb constitutive model was adopted for all rock strata, with a bulk density of 2.5 g/cm^3. According to the *in-situ* stress measurement results (Table 2), the lateral pressure coefficients in the x and y directions were set to 1.4 and 1.2, respectively. The mechanical parameters of each rock layer were assigned based on laboratory test results (Table 1). The initial stress field was balanced and calibrated in terms of magnitude and orientation prior to excavation. Subsequently, the working face was excavated, and the distribution range of abutment pressure around the face was obtained and compared with field observations to further calibrate the model, thereby improving the reliability of the simulation results.

3.2.2. Distribution Characteristics of Mining-Induced Stress

Under natural conditions, the coal-rock mass exists in a state of three-dimensional stress equilibrium, and its physical and mechanical properties remain relatively stable. However, mining-induced disturbances disrupt this original equilibrium, leading to stress redistribution, fracture propagation, and degradation of mechanical properties, which in turn result in deformation and instability of the surrounding rock.

A systematic numerical simulation was conducted to analyze the excavation process of a working face with a maximum width of 140 m in the No. 26 coal seam of the Baliancheng Coal Mine. The stress contours around the goaf and the distribution of advanced mining-induced stress in front of the working face are illus-

trated in Figure 7 and Figure 8, respectively.

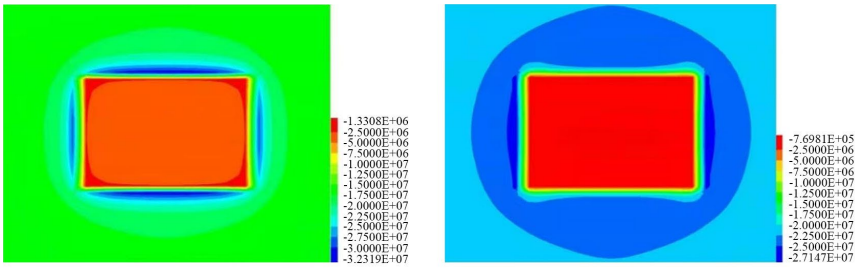

(a) Vertical stress (b) Horizontal stress

Figure 7. Stress contour map around the goaf of the No. 26 coal seam working face.

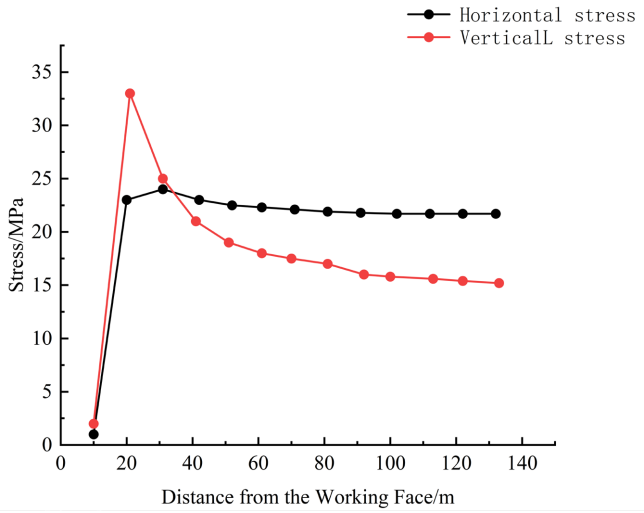

Figure 8. Advance abutment stress curve of the No. 26 coal seam working face.

After retreat mining of the coal seam working face, both the horizontal stress and the vertical stress in front of the working face exhibit an evolutionary trend characterized by an initial increase followed by a subsequent decrease, as shown in Figure 8. The specific characteristics are described as follows.

Variation characteristics of horizontal stress: Within the range of 0 - 30 m ahead of the working face, the horizontal stress shows a gradual increasing trend, reaching a peak value of 24.39 MPa, which is approximately 1.17 times the original *in-situ* stress. As the working face advances into the zone 30 - 130 m ahead, the horizontal stress gradually decreases, with values ranging from 22.11 to 24.39 MPa, corresponding to 1.06 - 1.17 times the original *in-situ* stress. Overall, the increase in horizontal stress is relatively limited, and its variation remains relatively gentle.

Variation characteristics of vertical stress: The vertical stress exhibits a more pronounced response to mining disturbance. In the zone 0 - 20 m ahead of the working face, the vertical stress increases progressively and reaches a peak value of 32.50 MPa, approximately 2.18 times the original *in-situ* stress. In the range of 20 - 130 m ahead of the working face, the vertical stress gradually decreases, varying between 16.52 and 32.50 MPa, equivalent to 1.11 - 2.18 times the original *in-*

situ stress. Notably, within the interval of 20 - 30 m ahead of the working face, the vertical stress remains at a relatively high level, ranging from 24.91 to 32.50 MPa (1.67 - 2.18 times the original *in-situ* stress), indicating that this zone is still strongly influenced by mining activities.

Comprehensive analysis: The results indicate that, in the advance zone of the No. 26 coal seam working face, the magnitude of vertical stress increase is significantly greater than that of horizontal stress, and its variation trend is more pronounced. Overall, the region most strongly affected by mining-induced stress is concentrated within 0 - 30 m ahead of the working face. In particular, the high vertical stress zone in this range provides an important reference for surrounding rock stability assessment and support design.

4. Stability Classification of Surrounding Rock in Roadways of Gently Inclined and Inclined Coal Seams

To ensure safe and normal production, roadways must maintain an adequate level of stability. According to the requirements of safety regulations and technical specifications, a roadway should retain its required geometry and cross-sectional dimensions throughout its service life.

4.1. Determination of Classification Indicators

Based on a comprehensive review of surrounding-rock classification methods both in China and abroad and targeted investigations, and considering practical applicability in production, a surrounding-rock stability classification scheme for retreat-mining roadways in gently inclined and inclined coal seams has been established in China; the corresponding classes and indices are summarized in Table 3.

Table 3. Classification of surrounding rock stability for retreat-mining roadways in gently inclined and inclined coal seams.

Category	Stability degree	Roof			Floor-Floor		Coal seam strength	Joints and Bedding	Average first-caving interval of the immediate roof, L (m)	Roof-floor	
		Rock type	Rock strength (MPa)	N	Rock type	Rock strength (MPa)				Convergence rate (%)	Convergence (mm)
I	Very Stable	Sandstone, Limestone,	68 - 120 average 96.5	0	Sandstone, Siltstone,	29 - 90 average 64.3	Medium-hard and	Not Developed	25	<5	<40
II	Stable	Sandy shale, Sandy mudstone	22.4 - 78 average 49.7	—	Sandy shale, Sandy mudstone, Mudstone	15 - 55 average35.3	1.25 - 2.7	Slightly Developed	15	5 - 10	
III	Moderately Stable	Shale, Sandy shale	10 - 110 average 45.8	0.4 - 8	Shale, SandyShale	10 - 110 average 45.8	Medium-hard 0.7 - 2.5	Moderately Devel	10	10 - 20	>200
IV	Unstable	Siltstone, mudstone, Shale	22 - 78 average 55.2	1 - 4	Siltstone, Sandy mudstone, Shale	12.4 - 55 average 1.88	Medium-hard 0.7 - 3.0	Developed	12	20 - 35	
V	Extremely Unstable	Mudstone, Shale	25 - 49 average 34.7	2.3 - 40	Mudstone, Shale	9 - 35 average 13.8	Soft 0.8 - 1.25	Developed	10	>35	

For a long time, roadway stability in coal mines has been evaluated largely through experience-based and qualitative (fuzzy) judgments, and unified quantitative criteria have been lacking. To scientifically characterize roadway stability, key classification indices were determined with reference to Qian's classic work on mine pressure and its control (Qian, 1991) and the study by Li and Hou on the characteristics and application of rock-bolt support in roadways (Li & Hou,2008). The selected indices include the strengths of the roof, floor, and coal seam (σD, σd, σM), roadway burial depth (H), first caving interval of the immediate roof(L), and the mining influence index (N) (Wang, 2015; Bai et al., 2020).

4.2. Selection Method of Classification Indicators

1) Three surrounding rock strength indicators (σ_roof, σ_coal, σ_floor): The uniaxial compressive strengths of the roof and floor rocks were determined as weighted average values within ranges equivalent to two times and one time the roadway width above the roof and below the floor, respectively. The uniaxial compressive strength of the coal seam was taken as the strength of the coal on both sides of the roadway. All strength values are expressed in MPa.

2) Roadway burial depth: The burial depth of the roadway refers to the vertical distance between the roadway location and the ground surface. For inclined roadways, the burial depth can be determined by segmented averaging. The unit is meters (m).

3) Rock mass integrity index (L): The rock mass integrity index is determined by converting the initial caving step distance of the immediate roof. The unit is meters (m).

4) Mining influence indicator (N): The mining influence refers to the effect of advanced abutment pressure induced by working face extraction. The mining influence coefficient is defined as the mining-induced stress concentration factor.

Based on comprehensive field investigations, *in situ* monitoring, and laboratory tests, the roof of the No. 26 seam roadway is predominantly a medium-hard composite strata composed of silty mudstone and argillaceous sandstone, with an average uniaxial compressive strength (UCS) of 51.37 MPa. The floor consists of a single medium-hard silty mudstone layer, with an average UCS of 50.63 MPa. The coal seam has a Protodyakonov coefficient of 0.90. The surrounding rock mass shows moderately developed fracturing. The ratio of the maximum horizontal principal stress to the vertical stress is 1.33, and the mining-induced stress concentration factor is 2.18. The average first weighting interval of the immediate roof is 14 m. The maximum roof-floor convergence is 290 mm, with a relative convergence of 11.15%. According to the classification table for surrounding-rock stability of recovery roadways in gently inclined and inclined coal seams (**Table 3**), the surrounding-rock stability at Baliancheng Coal Mine is classified as Class III (moderately stable), as listed in **Table 4**.

Table 4. Classification results of surrounding rock stability of mining roadways in baliancheng coal mine.

Roof			Floor		Coal seam strength	Joint bedding	Average initial caving interval of immediate roof L (m)	Roof-floor		Stability degree
Rock type	Rock strength (MPa)	N	Rock type	Rock strength (MPa)				Roof-floor convergence rate (%)	Roof-floor convergence amount (m)	
Sandy mudstone Argillaceous sandstone	49.60 - 53.14 average 51.37	2.18	Siltstone	50.63	0.90	Moderately developed	14	11.15	0 - 290	Moderately stable

5. Field Implementation of Support

5.1. On-Site Support Scheme

Given that the surrounding-rock stability of the No. 26 seam retreat-mining gateroad at Baliancheng Coal Mine was assessed as Class III (moderately stable), the original support system was systematically optimized to improve the integrity and load-bearing capacity of the support structure. In the original scheme, roof bolts were 2000 mm long with 5 bolts per row; cable bolts (anchor cables) were 6500 mm long with 3 cables per row; and rib bolts were 1800 mm long with 4 bolts per row.

According to borehole imaging observations, the roof strata are mainly a composite of silty mudstone and argillaceous sandstone. A thin coal interlayer of approximately 1.0 m is present. Within 0 - 2.0 m above the roofline, the rock mass is relatively fractured, forming a jointed zone dominated by transverse discontinuities. In the argillaceous sandstone, longitudinal fractures are developed at depths of 5.15 - 6.95 m. The coal on both ribs is relatively weak, with a Protodyakonov coefficient f = 0.9.

In the optimized scheme, the roof-bolt length was increased to 2200 mm with 6 bolts per row; the cable-bolt length was increased to 7300 mm with 3 cables per row; and the rib-bolt length was increased to 2000 mm with 4 bolts per row. The row spacing remained the same as that in the original scheme. The optimized support layout is shown in Figure 9 and Table 5.

Table 5. Parameters of roadway support design.

Stability class	Support scheme	Support type	Spacing and layout
Very stable (I)	rock-bolt support	Φ18 mm × 2000 mm smooth steel rock bolt Φ15.24 mm × 4500 mm cable bolts	Bolt spacing: 1000 mm × 1000 mm, 5 bolts per row; Cable spacing: 2000 mm × 2000 mm, 1 cable per row
Stable (II)	rock bolts + cable bolts	Φ18 mm × 2000 mm left-hand threaded steel rock bolt Φ15.24 mm × 4500 mm cable bolts	Bolt spacing: 900 mm × 1000 mm, 5 bolts per row; Cable spacing: 2000 mm × 2000 mm, 2 cables per row
Moderately stable (III)	rock bolts + cable bolts + wire mesh (combined support)	Φ20 mm × 2200 mm deformed steel rock bolt Φ17.8 mm × 7300 mm cable bolts 6.5 mm steel wire mesh	Bolt spacing: 800 mm × 1000 mm, 6 bolts per row; Cable spacing: 1200 mm × 2000 mm, 3 cables per row

Continued

Unstable (IV)	rock bolts + cable bolts + steel ladder + wire mesh (reinforced combined support)	Φ20 mm × 2200 mm left-hand threaded steel rock bolt Φ17.8 mm × 80000 mm cable bolts Q235Φ20 mm × 70 mm steel ladder 1050 mm × 4800 mm rhombic metal mesh	Bolt spacing: 800 mm × 900 mm, 7 bolts per row, with extended anchorage; Cable spacing: 1000 mm ×2000 mm, 4 cables per row
Extremely unstable (V)	rock bolts + cable bolts + steel ladder + wire mesh (reinforced combined support); additional steel sets installed if necessary	Φ14steel strap with reinforcement Φ20 mm × 2200 mm left-hand threaded steel rock bolt Φ17.8 mm × 9000 mm cable bolts Q235Φ20 mm × 70 mm steel ladder 1050 mm × 4800 mm rhombic metal mesh	Bolt spacing: 800 mm × 800 mm, 7 bolts per row, with extended anchorage; Cable spacing: 800 mm× 1000 mm, 5 cables per row

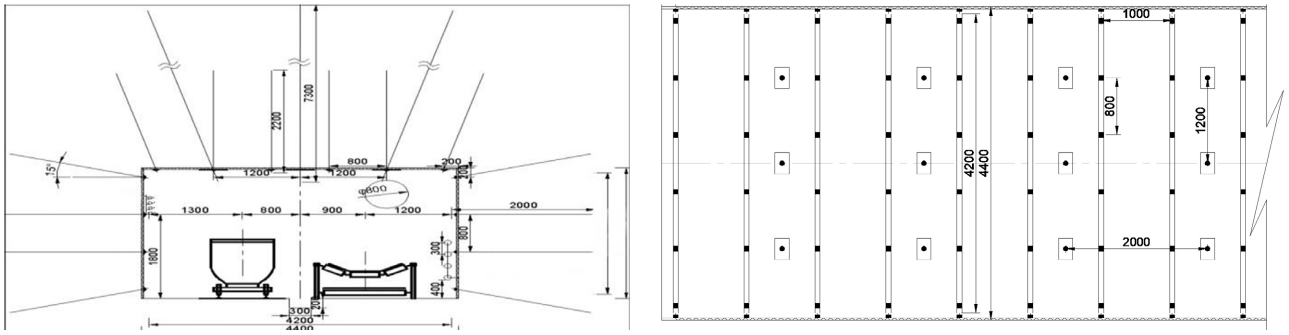

Figure 9. Roadway support cross-section.

5.2. Verification of Support Performance

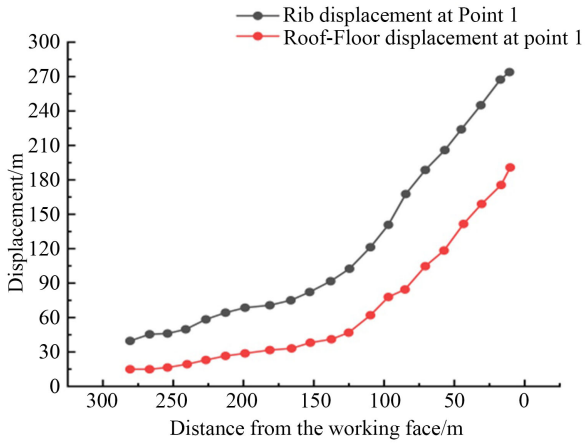

Figure 10. Displacement monitoring diagram of measuring point 1.

To evaluate the performance of the roadway support design, convergence monitoring was conducted during retreat mining by tracking the temporal evolution of roadway deformation, including roof-floor convergence and rib-to-rib convergence. A cross-measurement layout was adopted for convergence monitoring. Two monitoring stations were installed in the roadway. The deformation histories

recorded over approximately 40 days are shown in Figure 10 and Figure 11. The results indicate that, as the working face advanced, both roof-floor convergence and rib convergence at the two stations increased noticeably. In general, the ribs exhibited larger deformation amplitudes than the roof and floor. After the implementation of the optimized support, the convergences of both the roof-floor and the ribs decreased significantly, suggesting an evident reinforcement effect. Therefore, the surrounding-rock stability classification and the corresponding support design are proven to be effective for maintaining roadway stability.

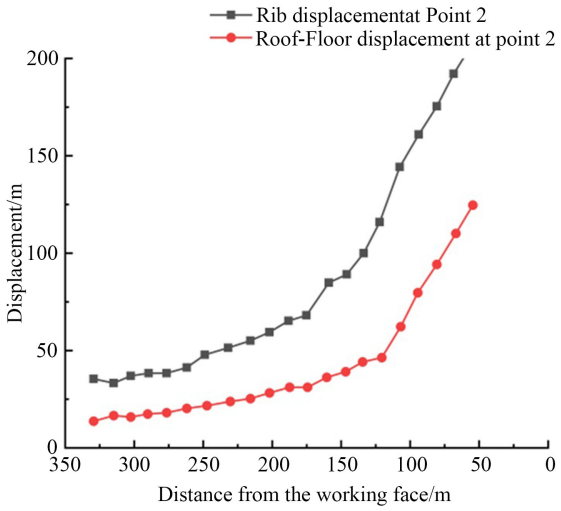

Figure 11. Displacement monitoring diagram of measuring point 2.

6. Conclusion

1) Based on *in situ* coring and drilling data, the roof of the No. 26 coal roadway at Baliancheng Coal Mine is identified as a medium-hard composite strata mainly composed of silty mudstone and argillaceous sandstone, whereas the floor consists of a single medium-hard silty mudstone layer. Laboratory rock-mechanics tests were conducted on core specimens to obtain a series of physical and mechanical parameters for the roof, floor, and coal-rock strata, providing the input basis for subsequent numerical modelling. *In situ* stresses were measured using the hydraulic fracturing method, yielding a maximum horizontal principal stress (S_H) of 14.07 - 18.69 MPa, a minimum horizontal principal stress (S_h) of 9.01 - 10.72 MPa, and a vertical principal stress (S_V) of 14.01 MPa. The ratio SH/SV is 1.33, indicating a horizontal-stress-dominated regime in the study area.

2) FLAC3D numerical simulations were performed to investigate the evolution of the mining-induced stress field during retreat mining of the No. 26 seam. The results indicate that the zone 0 - 30 m ahead of the working face is significantly influenced by mining-induced stresses. Within 0 - 20 m ahead of the face, the peak vertical stress reaches 32.50 MPa, approximately 2.18 times the initial vertical stress, which is substantially higher than the increment in horizontal stress; therefore, it is a key controlling factor for surrounding-rock stability evaluation and

support design.

3) Considering the geological-structural characteristics of the roadway, the physical and mechanical properties of the surrounding rock, and the *in situ* stress state, the principal controlling factors were identified, including roof/floor lithology, rock strength, coal strength, mining influence indices, rock-mass integrity indices, joint and fracture development, and roof-floor convergence. Referring to the stability classification table for retreat-mining gateroads in gently inclined and inclined coal seams, the surrounding-rock stability of the No. 26 retreat-mining gateroad at Baliancheng Coal Mine is classified as Class III (moderately stable).

4) The original support scheme was optimized by adjusting key parameters and enhancing the structural capacity. Field application demonstrates that the optimized support design can effectively control the deformation of the roof, floor, and ribs, achieving satisfactory support performance.

Conflicts of Interest

The authors declare no conflicts of interest regarding the publication of this paper.

References

Bai, D. D., Ji, Z., Li, P. et al. (2020). Evaluation and Prevention Technology of Impact Hazard Comprehensive Index Method in Semi-Isolated Working Face. *Coal Science and Technology, 48,* 188-193. (in Chinese) https://www.cnki.com.cn/Article/CJFDTotal-MTKJ2020S2037.htm

Ding, X. Q., Qiao, L., & Zhu, L. Y. (2009). Study on the Classification and Support of the Wall Rock of Mining Roadway Based on Fuzzy Clustering. *Metal Mine, 39,* 11-15. (in Chinese) http://www.jsks.net.cn/CN/Y2009/V39/I05/11

Dong, E. Y., Yuan, C., Li, M. et al. (2023). Study on Stability Analysis and Anchorage Optimization Design of Surrounding Rock in Soft Rock Roadway. *Coal Technology, 42,* 54-58. (in Chinese) https://doi.org/10.13301/j.cnki.ct.2023.09.011

Duan, Z. R. (2018). Study on the Stability Classification of Roadway Surrounding Rock Based on Fuzzy Clustering Analysis. *Coal, 27,* 15-17. (in Chinese)

Feng, R. G. (2022). *Stability Analysis of Surrounding Rock in Deep Roadway under Complex Stress Field*. Master's Thesis, Hebei University of Engineering. (in Chinese) https://doi.org/10.27104/d.cnki.ghbjy.2022.000280

Hou, C. J., Guo, L. S. et al. (1999). *Rock Bolting Support for Coal Roadways*. China University of Mining and Technology Press. (in Chinese)

Li, D. W., & Hou, C. J. (2008). Analysis and Application on Bolt Support Characteristic of Roadway. *Journal of China Coal Society, 6,* 613-618. (in Chinese) https://doi.org/10.13225/j.cnki.jccs.2008.06.008

Lian, X. Y., Li, J., Wu, Z. et al. (2023). Study on Fuzzy Cluster Analysis of Roadway Surrounding Rock Failure Theory. *China Coal, 49,* 37-45. (in Chinese) https://doi.org/10.19880/j.cnki.ccm.2023.06.006

Liu, H. T., Zhou, G. D., Han, Z. J. et al. (2024). Stability Analysis and Optimization Design of Roadway Surrounding Rock under Multiple Factors. *Journal of Mining Science and Technology, 9,* 504-518. (in Chinese) http://kykxxb.cumtb.edu.cn/en/article/Y2024/I4/504

Ma, Q. S., Zhao, X. Z., Song, Z. Q. et al. (2024). Design and System Application of Risk

Evaluation Model for Mining Roadway Stability. *Coal Mine Safety, 55,* 129-138. (in Chinese) https://doi.org/10.13347/j.cnki.mkaq.20231009

Qian, M. G. (1991). *Mine Pressure and Its Control*. Coal Industry Press. (in Chinese)

Wang, Y. S. (2015). *Intelligent Methods for Stability Classification of Roadway Surrounding Rock and Support Decision-Making*. PhD Thesis, Anhui University of Science and Technology. (in Chinese)

Xu, H. J. (2021). Discussion on Stability Classification of Surrounding Rock and Supporting Problems of Mining. *Energy and Energy Conservation, 55,* 36-37. (in Chinese) https://doi.org/10.16643/j.cnki.14-1360/td.2021.09.013

Yin, D. G. (2015). Influence of Relative Position of Deep Buried Fault and Roadway on Roadway Stability. *Shanxi Coking Coal Science & Technology, 39,* 49-52. (in Chinese)

Zhang, T. (2019). Analysis of Influencing Factors and Failure Forms of Surrounding Rock Stability in Mining Roadway. *Energy Technology and Management, 44,* 117-119. (in Chinese)

Zhang, T., Zhao, X., Zhu, G. P. et al. (2016). A Multi-Coupling Analysis of Mining-Induced Pressure Characteristics of Shallow-Depth Coal Face in Shendong Mining Area. *Journal of China Coal Society, 41,* 287-296. (in Chinese) https://doi.org/10.13225/j.cnki.jccs.2016.0113

Zhao, J. H., Li, F. J., Liu, Y. Z. et al. (2024). Stability Analysis and Support Research of Shaft and Roadway Surrounding Rock Based on Key Block. *China Mining Magazine, 33,* 304-311. (in Chinese)

Zhu, Y. J., Shi, H. Y., Wang, P. et al. (2015). Multiple Linear Regression Analysis on Affecting Factors of Tip-to-Face Roof Caving Height. *Journal of Hunan University of Science and Technology (Natural Science Edition), 30,* 1-6. (in Chinese) https://doi.org/10.13582/j.cnki.1672-9102.2015.03.001